Application of vermiculite-derived sustainable adsorbents for removal of venlafaxine

Andreia Silva[1] · Sílvia Martinho[1] · Wojciech Stawiński[1] · Agnieszka Węgrzyn[2] · Sónia Figueiredo[1] · Lúcia H. M. L. M. Santos[1] · Olga Freitas[1]

Abstract

Removal of emerging pollutants, such as pharmaceuticals, from wastewater is a challenge. Adsorption is a simple and efficient process that can be applied. Clays, which are natural and low-cost materials, have been investigated as adsorbent. In this work, raw vermiculite and its three modified forms (expanded, base, and acid/base treated) were tested for removal of a widely used antidepressant, venlafaxine. Adsorption kinetics followed Elovich's model for raw vermiculite while the pseudo-2nd order model was a better fit in the case of other materials. Equilibrium followed Langmuir's model for the raw and the acid/base-treated vermiculite, while Redlich-Peterson's model fitted better the expanded and the base-treated materials. The adsorption capacity of vermiculite was significantly influenced by the changes in the physical and chemical properties of the materials caused by the treatments. The base-treated, raw, and expanded vermiculites showed lower maximum adsorption capacities (i.e., 6.3 ± 0.5, 5.8 ± 0.7, 3.9 ± 0.2 mg g^{-1}, respectively) than the acid/base-treated material (33 ± 4 mg g^{-1}). The acid/base-treated vermiculite exhibited good properties as a potential adsorbent for tertiary treatment of wastewater in treatment plants, in particular for cationic species as venlafaxine due to facilitation of diffusion of the species to the interlayer gallery upon such treatment.

Introduction

The global community is becoming increasingly aware of both the environmental presence and the real or potential environmental impact of man-made chemicals. Continuous contamination of the environment with chemical compounds and their adverse effects on both ecosystems and human health are among the most relevant environmental issues of today (Kuzmanovic et al. 2013). According to European Inventory of Existing Commercial Chemical Substances (EINECS), in the European Union (EU), there are more than 100,000 registered chemicals of which 70,000 are in daily use (Kuzmanovic et al. 2013).

Pharmaceuticals are a large group of chemicals that are used daily in human and veterinary medicine. They represent one with the largest inputs to the environment and by far are the most extensive range of emerging contaminants reported to date. The excretion of pharmaceuticals (and metabolites) is a logical consequence of their consumption and constitutes the major source of entry into the environment, whereas discharges of unused medicines and effluents from manufacturing facilities are secondary (Eichhorn 2013). The presence of

[1]   REQUIMTE/LAQV, Instituto Superior de Engenharia do Porto, Rua Dr. António Bernardino de Almeida 431, 4200-072 Porto, Portugal

[2]   Faculty of Chemistry, Jagiellonian University, ul. Ingardena 3, 30-060 Kraków, Poland

pharmaceuticals in drinking water sources has now become an important water quality issue (Eichhorn 2013; Ferrer and Thurman 2013; Kuzmanovic et al. 2013). Although pharmaceuticals are present at low concentrations in the environment, their effects of exposure to multiple stressors on ecosystems are still unknown. Moreover, they occur in complex chemical mixtures and it has been found that mixtures might exhibit different effects than single compounds (Daughton 2013; Kümmerer 2008; Kuzmanovic et al. 2013). Whereas acute ecotoxicity effects at those levels of concentrations are not very probable, chronic effects can be more likely expected such as endocrine disruption, genotoxicity, and development of antibiotic-resistant pathogenic bacteria (Kuzmanovic et al. 2013).

Antidepressants are usually prescribed for long-term use; thus, they are produced in increased volumes compared to many other types of pharmaceuticals (Lambropoulou et al. 2017). A commonly used antidepressant, venlafaxine, and its major metabolite, O-desmethyl-venlafaxine, were shown to be present in various environment water samples (Bueno et al. 2012; de Jongh et al. 2012; Lajeunesse et al. 2012; Metcalfe et al. 2010; Papageorgiou et al. 2016; Schultz and Furlong 2008; Valcarcel et al. 2011). The degree of removal and biodegradation of pharmaceuticals during wastewater treatment varies considerably. Thus, the parent compounds and the associated transformation products may enter the environment since they are only partially eliminated by conventional wastewater treatment plants (Kuzmanovic et al. 2013). The presence of antidepressants at low concentrations (ngL^{-1}), which are present as a mixture in the aquatic environment, may induce chronic toxicity effects in the aquatic organisms (Santos et al. 2010). Among the various techniques of tertiary water treatment that can be applied for pharmaceutical removal, such as membrane filtration, advanced oxidation processes, and adsorption, the last has been proven to be superior to other techniques for a variety of reasons, including simplicity of design, easy operation, low operation cost, high removal efficiency, possibility of adsorbent regeneration, and wide range of applications. Therefore, it is considered one of the most promising, effective, and attractive approach for tertiary water treatment (Gupta and Ali 2012; Teng and Low 2012). Activated carbon is an industrially produced material with broad applications and high removal efficiencies; however, its application is restricted due to high costs (Gupta and Ali 2012; Teng and Low 2012; Worch 2012). Therefore, there is a need to search for cheaper alternatives. Clays show good perspectives in this field owing to their low cost, large specific surface area, excellent physical and chemical stability, and other advantageous structural and surface properties (Teng and Low 2012; Worch 2012).

Although there are a few studies where clays have been used as adsorbents to remove pharmaceuticals (Table 1), the application of vermiculite in this field is not yet properly investigated. There is also one preliminary study by Styszko et al. (2015) who tested several clays, including exfoliated vermiculite, for removal of ibuprofen, diclofenac, ketoprofen, carbamazepine, and triclosan.

The aim of this study was application of raw and expanded vermiculite together with two previously developed vermiculite-based adsorbents obtained on a way of acid-base and the base treatment for removal of venlafaxine from aqueous solution. The modified materials were extensively tested in adsorption of heavy metals and dyes and showed significantly increased maximum adsorption capacity (Stawiński et al. 2017b); thus, they can also find application in remediation of wastewater laden with pharmaceuticals. Moreover, to the authors' best knowledge, such application has not been reported in the literature.

Materials and methods

Reagents

Venlafaxine was used in the form of venlafaxine hydrochloride, purity ≥ 98% (Sigma-Aldrich, Steinheim, Germany). Its main properties are depicted in Table 2. HPLC-grade methanol (MeOH), HPLC-grade acetonitrile, and formic acid, purity 99–100% (VWR Chemicals BDH Prolabo, PA, USA). HPLC-grade water was obtained from purification of deionized water in a Millipore Simplicity 185 System (Darmstadt, Germany). Venlafaxine stock standard solution was prepared by dissolving an appropriate amount of the reagent in methanol and stored at − 20 °C.

Adsorbents

Raw vermiculite (W) and its expanded version (Ve), in commercially available form, widely used in various fields (e.g., civil engineering, farming), were supplied by Rominco Polska Sp. z o.o. (Krakow, Poland). Treated materials included a base-treated raw vermiculite (WNaOH) and an acid/base-activated raw vermiculite (WN-OH). WNaOH was prepared by mixing of a weighted portion of W with 2 mol L^{-1} sodium hydroxide solution, in proportion of 1 g of W for each 100 mL of the solution, at room temperature under constant stirring for 4 h. WN-OH was prepared from W by boiling it at 98 °C under constant stirring in a round bottom flask equipped with a condenser, for 2 h in 1.8 mol L^{-1} nitric acid solution (1 g of W for each 100 mL of acid solution), then a washing in 10% citric acid solution was performed under stirring for 2 h, which was followed by stirring for 1 h in 0.5 mol L^{-1} sodium hydroxide solution (Stawinski et al. 2016). Table 3 presents selected properties of these materials. Detailed characterization of each material on each step of the treatment can be found in

Table 1 Application of clay minerals in remediation of water polluted with pharmaceuticals

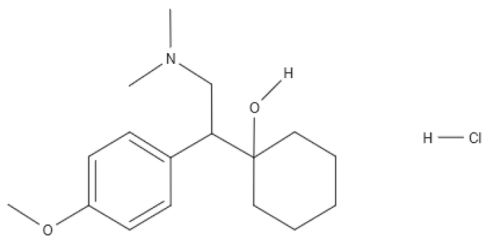| Pharmaceutical	Materials used	Adsorption capacity ($mol\ g^{-1}$)	Reference
Tramadol Doxepin	Smectite	0.8×10^{-3} 10^{-3}	Thiebault et al. (2015)
Ciprofloxacin	Montmorillonite	1.19×10^{-3}	Wang et al. (2011)
	Rectorite	4.1×10^{-4}	
	Illite	10^{-4}	
	Birnessite	2.2×10^{-4}	Jiang et al. (2013)
Tetracycline	Illite	7.2×10^{-5}	Chang et al. (2012)
	Montmorillonite	1.04×10^{-3}	Li et al. (2010a)
	Kaolinite	9.0×10^{-6}	Li et al. (2010b)
	Rectorite Palygorskite	3.15×10^{-4} 2.1×10^{-4}	Chang et al. (2009)
Amitriptyline	Palygorskite	1.68×10^{4}	Tsai et al. (2016)
Enrofloxaxin	Kaolinite Montmorillonite	5.52×10^{-5} 6.41×10^{-4}	Rivagli et al. (2014)
		6.67×10^{-4}	Wan et al. (2013)
	Illite	2.28×10^{-4}	
	Kaolinite	2.0×10^{-5}	
Ranitidine	Palygorskite	1.56×10^{-4}	Li et al. (2016)
Diphenhydramine	Montmorillonite	8.8×10^{-4}	Li et al. (2011)
Gemfibrozil Mefenamic acid Naproxen	Exfoliated vermiculite	4.2×10^{-6} 2.85×10^{-7} 8.38×10^{-6}	Dordio et al. (2017)

the following publications: Stawiński et al. (2016), Stawiński et al. (2017a), and Stawiński et al. (2017b).

The structure of the fresh and saturated materials was studied by analysis of XRD patterns recorded using an X-ray powder diffractometer (Bruker, D2 PHASER) equipped with $CuK\alpha$ radiation source.

Determination of venlafaxine concentration

The quantification of venlafaxine was performed by high-performance liquid chromatographic analysis with fluorescence detection (HPLC-FLD) using a Shimadzu LC Prominence (Shimadzu Corporation, Kyoto, Japan) equipped

Table 2 Physico-chemical properties of venlafaxine hydrochloride

Property		Reference
Formula	$C_{17}H_{27}NO_2 \cdot HCl$	
Structure		
M_w ($g\ mol^{-1}$)	313.86	Sigma-Aldrich
S_w ($mg\ mL^{-1}$)	0.23	DrugBank
pKa	8.91; 14.42	DrugBank
log K_{ow}	2.69	Sigma-Aldrich

M_w molecular weight, S_w water solubility, pKa logarithm of the acid dissociation constant, $log\ K_{ow}$ logarithm of the octanol-water partition coefficient

Table 3 Physical and chemical properties of adsorbent materials (adapted from Stawinski et al. 2016)

Property	W	Ve	WNaOH	WN-OH
S_{BET} (m^2 g^{-1})	21	9	18	45
Pores volumes (cm^3 g^{-1})				
V_{meso}	2.84×10^{-3}	2.94×10^{-4}	1.12×10^{-2}	3.34×10^{-3}
V_{micro}	2.06×10^{-3}	4.28×10^{-4}	1.93×10^{-3}	1.05×10^{-3}
CEC (mmol 100 g^{-1})	93	38	97	44
pH_{pzc}	8.1	n.a.	n.a.	7.9
Chemical composition (weight %)				
MgO	23.3	n.a.	24.0	3.1
Al$_2$O$_3$	12.2	10.3	12.0	39.4
Fe$_2$O$_3$	9.7	10.4	11.0	10.4
SiO$_2$	58.0	31.7	52.0	43.3

S_{BET} Brunauer, Emmett, and Teller specific surface area; V_{meso}, volume of mesoporous; V_{micro}, volume of microporous; *CEC*, cation exchange capacity; pH_{pzc}, point of zero charge; *n.a.*, not analyzed

with a LC-20AB pump, a DGU-20A5 degasser, a SIL-20A autosampler, a CTO-20AC column oven, and a RF-10A-XL fluorescence detector (FLD). The control of the chromatographic system and the acquisition and processing of chromatographic data were made using LC solution version 1.25 SP2 software.

The chromatographic separation was achieved in a Luna C18 (4.6 × 150 mm, 5 μm) column (Phenomenex, USA). The mobile phase consisted in ultrapure water containing 0.1% formic acid (eluent A) and acetonitrile (eluent B). Samples were eluted using the following gradients: 0 min, 10% B/90% A; 0–7 min, increase from 10 to 80% B; 7–10 min, return to initial conditions (10% B/90% A); 10–14 min, equilibration of the column. The flow rate was 1 mL min^{-1} and the column was maintained at 35 °C. The injection volume was 20 μL. The excitation and emission wavelengths were 274 and 610 nm, respectively. The run time was 14 min and venlafaxine had a retention time of 4.47 min. Estimated limits of detection and quantification were 23.4 and 78.2 μg L^{-1} of venlafaxine, respectively.

Batch adsorption experiments

Kinetic and equilibrium experiments were carried out at room temperature (20 °C), with constant stirring at 400 rpm (Digital Ceramic Hot Plate Stirrer–AREC with VTF Digital Thermoregulator, VELP Scientifica, Italy). The pH was monitored from the initial value, close to 6, up to the final value, around 7.

In the kinetic experiments, weighted portions of 300 mg of W and Ve, and of 100 mg in the case of WNaOH and WN-OH, were placed in beakers and mixed with 250 mL of 883.9 μg L^{-1} aqueous solution of venlafaxine for 130 min. Samples were collected at determined time intervals, immediately centrifuged for 10 min at 9000 rpm (Heraeus Fresco 21 Microcentrifuge, Thermo Scientific, USA), and the

concentration of venlafaxine in the supernatants was determined by HPLC-FLD.

In the equilibrium experiments, portions of 30 mg of W and Ve, and 10 mg, in the case of WNaOH and WN-OH, were stirred for 60 min (time enough to reach equilibrium) in Erlenmeyer flasks with 20 mL of venlafaxine aqueous solution of concentrations varying from 100 to 15,000 μg L^{-1}. In the next step, the samples were centrifuged and the concentration of venlafaxine was determined as described above.

The adsorption capacity of the materials was calculated according to Eq. 1:

$$q_t = (C_0 - C_t) \cdot V/m \qquad (1)$$

where C_0 (μg L^{-1}) and C_t (μg L^{-1}) are the initial and time t (min) venlafaxine concentrations, respectively, V (L) is the volume of venlafaxine solution at time t and m (g) is the adsorbent mass.

After each experiment, the saturated materials were collected, washed with water in 5 cycles of mixing and centrifugation, and left to dry overnight at 40 °C; then, they were characterized by X-ray diffraction.

Data analyses

Kinetic and equilibrium parameters were estimated by non-linear regression. Considering the stirring speed used during the experiments, sufficient to eliminate the external resistance to mass transfer, the influence of external film diffusion was neglected. Three kinetic models were adjusted to the experimental data: pseudo-1st order model (Lagergren 1898), pseudo-2nd order model (Ho 2004), and Elovich's model (Low 1960). Experimental equilibrium results were fitted by the five following isotherm models: Freundlich's model (Freundlich 1906), Langmuir's model (Langmuir 1918), Sips' model (Sips 1948), Redlich-Peterson's model (Redlich

and Peterson 1959), and Tóth's model (Tóth 1971). Models' equations are presented in the "Supplementary Materials.^

Results

X-ray diffraction studies

The interlayer hydration complexes of clay minerals arise from intercalation of a discrete number of water layers. This number ranges from 0 to 3, corresponding to zero-, one-, two-, or three-layer hydrates. One of the main factors affecting the interlayer hydration is the interlayer cation and its polarization energy (Brigatti et al. 2006). Generally speaking, divalent interlayer cations tend to form two- and three-layer hydrates, while monovalent cations are hydrated with one water layer (Sposito and Prost 1982). Moreover, the hydration states change upon thermal treatment of the materials (Marcos et al. 2003). The XRD pattern of the raw vermiculite (W) exhibited characteristic d_{002} reflection corresponding to the interlayer space height, ascribed to the presence of double water layer in interlayer galleries accompanying the charge-balancing cations (Fig. 1a). In the expanded material (Ve), a series of reflections corresponding to the presence of double, single, and zero water layers were identified (Fig. 1b). The peak at the pattern of the material treated with acid and base (WN-OH) might be attributed to a new phase, saturated with Mg (Sakharov et al. 1999), composed of smectite-like layers and hydroxy-intercalated

vermiculite (HIV) formed due to migration of metal ions from the active dissolution of sites into the interlayer space (Kalinowski and Schweda 2007; Mareschal et al. 2009) (Fig. 1c). The reflection of the material treated with base (WNaOH) may be attributed to a phase originating from two- (Mg-vermiculite) and one-sheet (Na-vermiculite) (Huo et al. 2012) layers of water (Collins et al. 1992; Marcos et al. 2003; Ruiz-Conde et al. 1996) and interstratification between contracting and non-contracting phases (Walker 1961) (Fig. 1d). After saturation of the adsorbents, the peaks shifted towards lower angles, and in the case of the material Ve, the reflection at 1.025 nm had decreased its intensity.

Kinetic studies

The data gathered during the kinetic experiments with fitted models are presented in Fig. 2. Estimated kinetic parameters and results of statistical analysis are shown in Table 4. The kinetic profiles showed that equilibrium was reached within around 15 min in the case of the materials Ve and WN-OH, and in approximately 40 min in the case of WNaOH and W. The pseudo-2nd order model was the best fit for the first three materials; however, the results for W were better fitted by the Elovich's model. The kinetic constant (k_2) for the material Ve was the highest, followed by that for the materials W, WN-OH, and WNaOH. The latter one had the parameter an order of magnitude lower than that of the other adsorbents. In order to ease their comparison, the kinetic parameters were analyzed
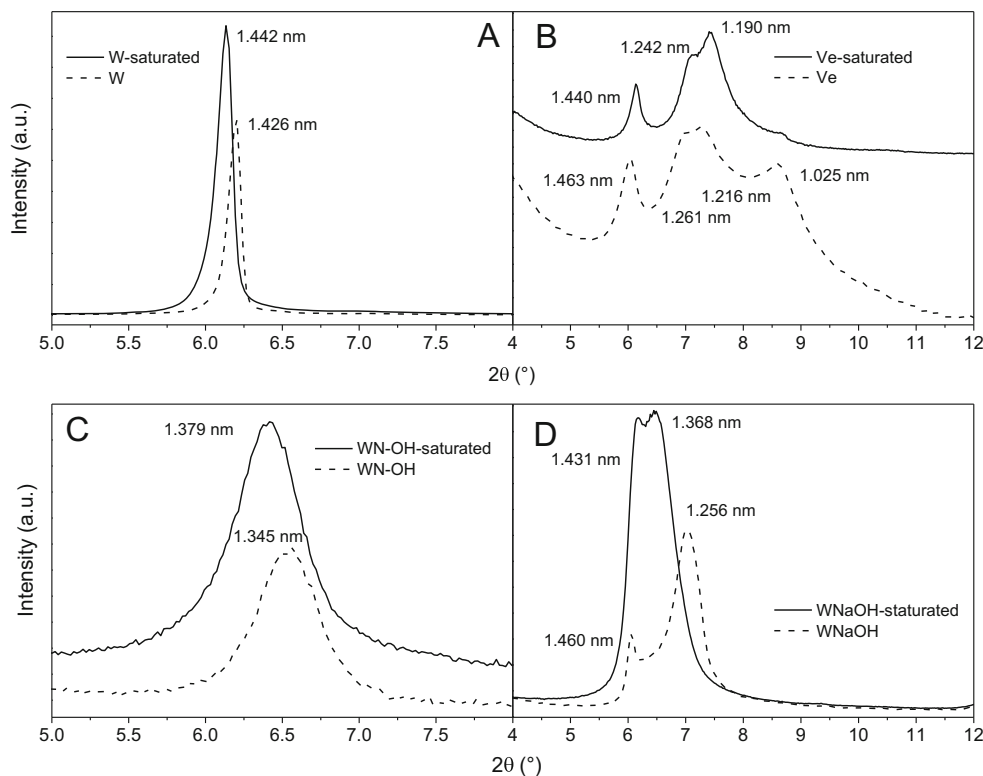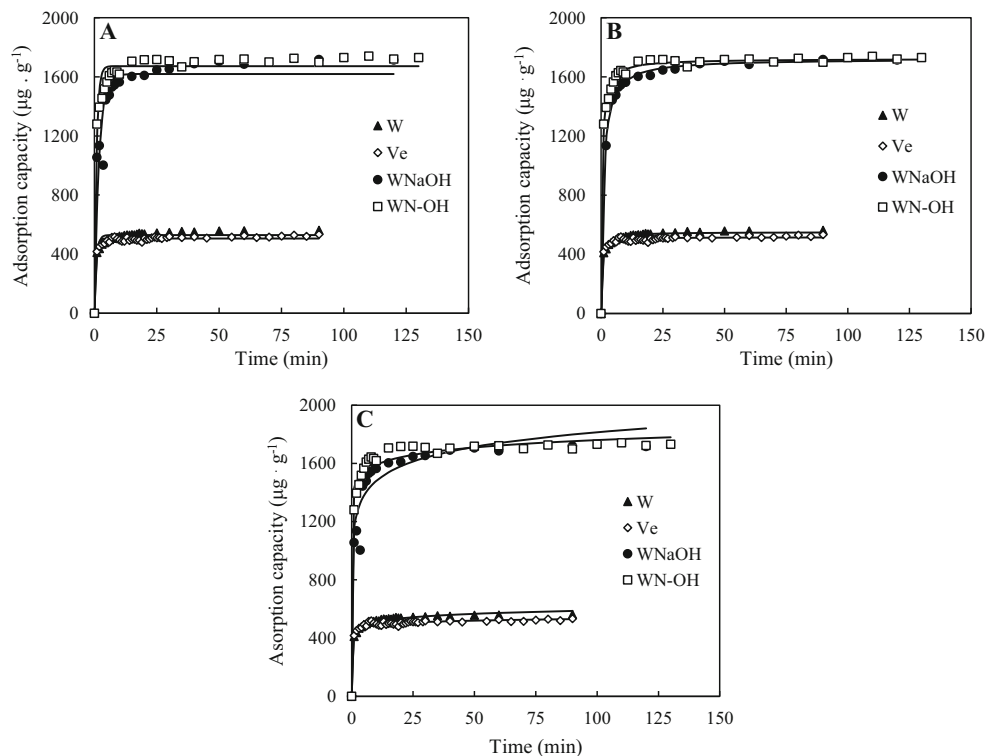

Fig. 1 XRD patterns of fresh and saturated with VLF raw (**a**), expanded (**b**), acid-base-treated (**c**), and base-activated (**d**) vermiculites

Fig. 2 Kinetic experimental data with fitted models: pseudo-1st order model (**a**), pseudo-2nd order model (**b**), and Elovich's model (**c**), for adsorption of VLF onto W, Ve, WNaOH, and WN-OH

according to the results of fitting of the pseudo-2nd order model for all adsorbents.

Equilibrium studies

The results of the equilibrium studies for the four investigated systems containing VLF and W, Ve, WNaOH, and WN-OH together with the fitted models are presented in Fig. 3. Estimated models' parameters and results of statistical analysis

are gathered in Table 5. Adsorption of VLF onto the raw (W) and acid-base-treated material (WN-OH) followed the Langmuir's model, whereas the Redlich-Peterson's isotherm equation was a better fit in the case of the expanded vermiculite (Ve) and in the base-treated material (WNaOH). According to the Langmuir's model, the material WN-OH showed the highest adsorption capacity, 33 ± 4 mg g^{-1}. The materials WNaOH and W were characterized by statistically similar removal efficiencies, 6.3 ± 0.5 and 5.8 ± 0.7 mg g^{-1}, respectively, and the lowest adsorption

Table 4 Kinetic parameters determined for the systems venlafaxine/W, Ve, WNaOH, and WN-OH and the respective statistical analysis

Material	Kinetic model	Parameters				Statistical analysis			
						R^2	s	χ^2_{red}	AIC
W	Pseudo-1st order	q_e	529 ± 5	k_1	1.2 ± 0.1	0.946	24.8	6.13×10^2	2.898
	Pseudo-2nd order	q_e	550 ± 3	k_2	0.0040 ± 0.0003	0.990	10.7	1.14×10^2	2.166
	Elovich	α	$1.21 \times 10^7 \pm 0.99 \times 10^7$	β	0.029 ± 0.002	0.991	10.2	1.03×10^2	2.125
Ve	Pseudo-1st order	q_e	505 ± 3	k_1	1.6 ± 0.1	0.964	15.6	2.44×10^2	2.464
	Pseudo-2nd order	q_e	515 ± 2	k_2	0.007 ± 0.001	0.984	10.5	1.10×10^2	2.117
	Elovich	α	$1.9 \times 10^{12} \pm 5.1 \times 10^{12}$	β	0.056 ± 0.006	0.981	11.4	1.30×10^2	2.191
WNaOH	Pseudo-1st order	q_e	1619 ± 38	k_1	0.54 ± 0.08	0.888	137.9	1.90×10^4	4.434
	Pseudo-2nd order	q_e	1723 ± 7	k_2	0.00060 ± 0.00003	0.998	17.6	3.10×10^2	2.594
	Elovich	α	$3.8 \times 10^5 \pm 5.0 \times 10^5$	β	0.007 ± 0.001	0.929	109.5	1.20×10^4	4.233
WN-OH	Pseudo-1st order	q_e	1672 ± 16	k_1	1.1 ± 0.1	0.956	73.2	5.35×10^3	3.848
	Pseudo-2nd order	q_e	1723 ± 7	k_2	0.0014 ± 0.0001	0.994	27.1	7.34×10^2	2.985
	Elovich	α	$1.9 \times 10^{10} \pm 4.5 \times 10^{10}$	β	0.014 ± 0.001	0.975	55.2	3.05×10^3	3.604

q_e (µg g^{-1}); α (µg g^{-1} min^{-1}); k_1 (min^{-1}); k_2 (g µg^{-1} min^{-1}); β (µg g^{-1})

Fig. 3 Equilibrium experimental data with fitted models: Freundlich's model (**a**), Langmuir's model (**b**), Sips' model (**c**), Redlich-Peterson's model (**d**), and Tóth's model (**e**) for adsorption of VLF onto W, Ve, WNaOH, and WN-OH
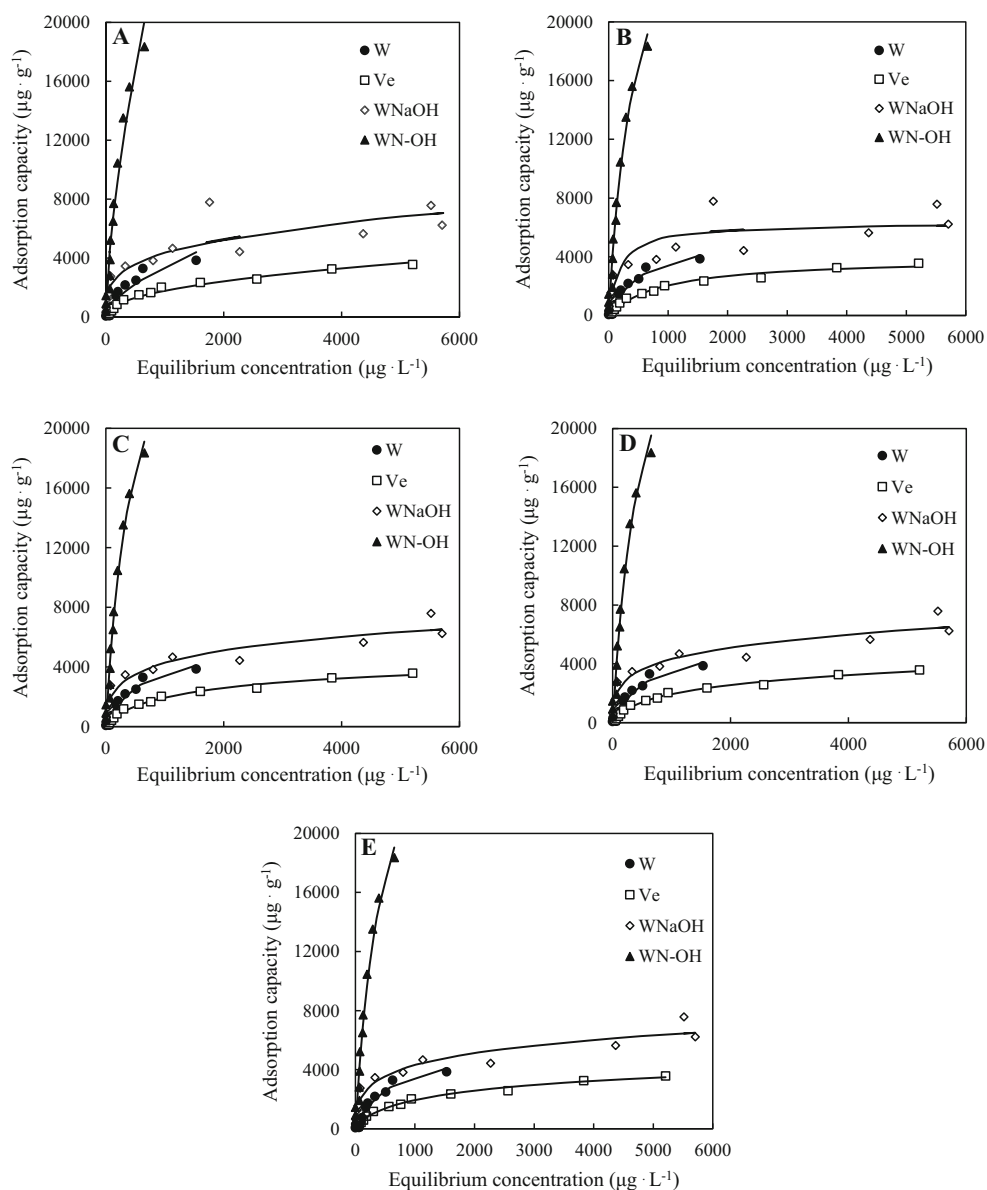
capacity, 3.9 ± 0.2 mg g^{-1}, was verified for Ve. All fitted isotherms had L-type configuration which suggests high affinity of VLF to the studied adsorbents. Additionally, VLF exhibits a low solubility in water (S_w), 0.23 mg mL^{-1}, and has a high octanol-water partition coefficient value (log K_{ow}), 2.69 (Table 2), which favors the adsorption of this pharmaceutical.

A slight increase in pH of the solutions was noticed in all investigated systems. Initial pH was around 6 and increased about 1 during the adsorption experiments. In this range of pH, venlafaxine is positively charged (Table 2).

Discussion

The adsorption properties of studied materials are strongly dependent on their treatment method. The expanded

vermiculite (Ve), during its exfoliation, was subjected to high temperatures. Such process causes various changes in the material: a decrease in its specific surface area, dehydroxylation of its structure (Barshad 1950; Walker 1961) depriving the material of adsorption sites, and a significant loss of cation exchange capacity that can decrease almost to zero (Földvári 2011; Stefanova 2001). Owing to that, adsorption on Ve was very low. In this case, based on these facts and on the results of the kinetic experiments, it may be supposed that adsorption took place mostly on the external surface of the mineral, as it should be expected the migration of the relatively large pharmaceutical molecule would require longer time to be completed, especially for very low concentrations of the compound (low driving force of the process). Consequently, the adsorption process was completed faster, and therefore the kinetic parameter is high. The changes visible in the XRD pattern

Table 5 Isotherm parameters determined for the four systems venlafaxine/W, Ve, WNaOH, and WN-OH and the respective statistical analysis

Material	Isotherm model	Parameters						Statistical analysis			
								R^2	s	χ^2_{red}	AIC
W	Freundlich	n	1.6 ± 0.2	k_F	51 ± 26			0.883	453.2	2.05×10^5	5.531
	Langmuir	q_m	$5.8 \times 10^3 \pm 0.7 \times 10^3$	k_L	0.0016 ± 0.0004			0.949	299.8	8.99×10^4	5.173
	Sips	n_S	1.0 ± 0.2	q_m	$5.8 \times 10^3 \pm 1.7 \times 10^3$	k_S	0.002 ± 0.001	0.949	313.2	9.81×10^4	5.316
	Redlich-Peterson	β	1.0 ± 0.4	k_{RP}	9 ± 3	a_{RP}	0.002 ± 0.005	0.949	313.2	9.81×10^4	5.315
	Tóth	n_T	1.0 ± 0.7	q_m	$5.8 \times 10^3 \pm 2.6 \times 10^3$	b_T	637 ± 2770	0.949	313.2	9.81×10^4	5.315
Ve	Freundlich	n	2.2 ± 0.1	k_F	81 ± 18			0.973	193.7	3.75×10^4	4.809
	Langmuir	q_m	$3.9 \times 10^3 \pm 0.2 \times 10^3$	k_L	0.0011 ± 0.0001			0.981	161.5	2.61×10^4	4.674
	Sips	n_S	0.75 ± 0.09	q_m	$5.1 \times 10^3 \pm 0.8 \times 10^3$	k_S	0.0005 ± 0.0002	0.989	132.1	1.75×10^4	4.589
	Redlich-Peterson	β	0.77 ± 0.06	k_{RP}	7 ± 2	a_{RP}	0.01 ± 0.01	0.992	112.8	1.27×10^4	4.452
	Tóth	n_T	0.5 ± 0.2	q_m	$6.5 \times 10^3 \pm 2.0 \times 10^3$	b_T	26 ± 28	0.990	122.2	1.49×10^4	4.522
WNaOH	Freundlich	n	3.6 ± 0.6	k_F	$6.4 \times 10^2 \pm 2.4 \times 10^2$			0.862	996.5	9.93×10^5	6.216
	Langmuir	q_m	$6.3 \times 10^3 \pm 0.5 \times 10^3$	k_L	0.005 ± 0.003			0.855	1022.3	1.05×10^6	6.238
	Sips	n_S	0.4 ± 0.1	q_m	$1.4 \times 10^4 \pm 1.3 \times 10^4$	k_S	0.0001 ± 0.0004	0.948	592.6	3.51×10^5	5.828
	Redlich-Peterson	β	0.78 ± 0.05	k_{RP}	$1.6 \times 10^2 \pm 1.4 \times 10^2$	a_{RP}	0.2 ± 0.2	0.956	548.1	3.00×10^5	5.760
	Tóth	n_T	0.2 ± 0.2	q_m	$2.9 \times 10^4 \pm 5.7 \times 10^4$	b_T	1 ± 1	0.950	578.6	3.35×10^5	5.807
WN-OH	Freundlich	n	1.5 ± 0.1	k_F	287 ± 102			0.952	1357.1	1.84×10^6	6.484
	Langmuir	q_m	$3.3 \times 10^4 \pm 0.4 \times 10^4$	k_L	0.0022 ± 0.0005			0.974	1006.6	1.01×10^6	6.225
	Sips	n_S	1.0 ± 0.2	q_m	$3.2 \times 10^4 \pm 1.3 \times 10^4$	k_S	0.002 ± 0.002	0.974	1051.7	1.11×10^6	6.368
	Redlich-Peterson	β	1.0 ± 0.5	k_{RP}	71 ± 20	a_{RP}	0.002 ± 0.007	0.973	1061.9	1.13×10^6	6.376
	Tóth	n_T	1.0 ± 0.8	q_m	$3.3 \times 10^4 \pm 2.1 \times 10^4$	b_T	$0.5 \times 10^3 \pm 2.1 \times 10^3$	0.974	1053.4	1.11×10^6	6.369

n (dimensionless); q_m ($\mu g\ g^{-1}$); n_S (dimensionless); β (dimensionless); n_T (dimensionless); k_F ($\mu g\ g^{-1}\ (L\ \mu g^{-1})^{1/n}$); k_L ($L\ \mu g^{-1}$); k_{RP} (($\mu g\ g^{-1}$)($L\ \mu g^{-1}$)); k_S ($L\ \mu g^{-1}$); a_{RP} ($L\ \mu g^{-1}$)$^\beta$; b_T ($\mu g\ L^{-1}$)

after adsorption should be associated with disappearance of the zero water layer phase due to hydration of the material (the water molecule is considerably smaller than the molecule of VLF, thus it can easily migrate into the interlayer gallery of the clay mineral) (Marcos et al. 2009), rather than intercalation of VLF between the material's layers. It cannot be unambiguously stated that no VLF molecule was intercalated into the interlayer space; however, this phenomenon was not reflected in the XRD patterns thus no increase in the interlayer distance occurred. Moreover, it is likely that adsorption capacity has also been influenced by the loss of some meso- and microporosity (Haul 1982), from 2.84×10^{-3} (W) to $2.94 \times 10^{-4}\ cm^3\ g^{-1}$ (Ve) and 2.06×10^{-3} (W) to $4.28 \times 10^{-4}\ cm^3\ g^{-1}$ (Ve), respectively.

The adsorption capacity of the raw (W) and the base-treated material (WNaOH) reached a similar level. These materials have comparable specific surface areas, cationic exchange capacity (Table 3), and chemical composition; hence, there is no difference in the maximum adsorption capacity. However, there was a significant discrepancy between the values of the kinetic parameters, which was lower on the latter material. This phenomenon might be attributed to the fact that during base activation, exchangeable Mg^{2+} cations present in the interlayer gallery were exchanged by Na^+ (Stawiński et al.

2017b). Sodium having lower polarizing power is easier to exchange by another species than magnesium. Although there was a slight shift of the d_{002} reflection in the case of W after saturation, it should be rather attributed to varying the number of interlayer water molecules that do not cause any changes in the hydration state (Ferrage et al. 2005) than to intercalation of the adsorbate. It is possible, therefore, that the adsorption occurred essentially on the external surface of vermiculite, in particular in the structural hydroxyl groups located on the surface and at its broken edges (Schoonheydt and Johnston 2006). However, the longer time to reach equilibrium may suggest that some of the VLF is adsorbed via the mechanism of ion exchange with interlayer cations. On the other hand, in the case of WNaOH, the reflection present in the pattern of the unsaturated material at 1.265 nm shifted to 1.368 nm (Fig. 1), which may be interpreted as intercalation of the adsorbate between the layers. Such process is more time consuming, thus the adsorption rate is lower and the time to achieve equilibrium is also longer when compared to the material Ve and WN-OH.

The material subjected to acid-base treatment exhibited the best adsorption properties, and moderate adsorption rate. Also, in this case, the shift of the reflection in the XDR pattern (Fig. 1) may be associated with intercalation of VLF between

material's layers. The first step of this modification comprised acid activation. In the course of this process, some of the interlayer cations and metal cations from the octahedral layers were leached, causing formation of highly distorted material's structure. These changes resulted in a decrease in crystallinity and cationic exchange capacity, delamination of the layer structure, weakening of interaction between the layers, and formation of new adsorption sites on amorphous silica that cross-links the material giving it a "house of cards" structure (Stawiński et al. 2016). Nonetheless, this new amorphous phase also acted as a cementing agent impeding good dispersion of the material in solution, and it also clogged the entrance between the layers, rendering some of the adsorption sites inaccessible (Fernandes et al. 2007; Kaviratna and Pinnavaia 1994; Stawiński et al. 2016). Base treatment promotes the leaching of silicon and aluminum species from the mineral surface (Jozefaciuk et al. 2002; Kunze 1965). When such prepared material entered into contact with NaOH, the amorphous cementing phase was dissolved, the entrance to the interlayer was opened, and moreover, the remaining interlayer cation exchanged to Na^+. This subsequent treatment left a material that had decreased cationic exchange capacity, which facilitates migration of the species between layers, with Na^+ interlayer cations that are easier to exchange, and without amorphous silica causing a spherical obstruction. This material had also an increase in the specific surface area due to possible formation of surface cracks and voids, and by accumulation of iron and magnesium hydroxides (Jozefaciuk et al. 2002).

The slight increase in the pH of the solutions during the equilibrium experiments can be explained by adsorption of H^+ onto the structure of adsorbents (e.g., unsaturated bonds on the "broken edges"). Nonetheless, the final pH was lower than pKa of VLF, thus the molecule was protonated, and hence its interaction with the adsorbent surface enhanced.

Conclusions

Adsorption of venlaflaxine (VLF) on a natural clay mineral vermiculite (W), its thermally expanded version (Ve), and two other adsorbents derived from W, by base (WNaOH) and acid-base activation (WN-OH), have been tested. The adsorption kinetics followed the pseudo-2nd order model in all cases except for W, where Elovich's model was a better fit. The process was fast and was completed in approximately 15 min on Ve and WN-OH, and in around 40 min on WNaOH and W. Regarding equilibrium, the Langmuir's isotherm model represented the adsorption on W and WN-OH, whereas Redlich-Peterson's equation was the best fit for Ve and WNaOH.

The raw vermiculite reached a maximum adsorption capacity of 5.8 ± 0.7 mg g^{-1}; and after base activation, no significant change in the capacity was observed. Thermal treatment of the material resulted in deterioration of its adsorption capacity that decreased to 3.9 ± 0.2 mg g^{-1}. However, subsequent acid-base activation increased the capacity by 550% in relation to the starting vermiculite, reaching 33 ± 4 mg g^{-1}. This is a result of changes occurring in the material's structure (i.e., leaching of the layers, lowering the cation exchange capacity, and dissolution of the amorphous phase created during acid activation) that enable the whole interlayer space for adsorption of species.

The acid-base-treated vermiculite, so far, has been applied only for removal of metal cations and cationic dyestuffs from aqueous solution. This study proves that such adsorbents may be successfully applied for removal of other species from wastewater opening new perspectives for removal of pharmaceuticals.

References

Barshad I (1950) The effect of interlayer cations on the expansion of the mica type of crystal lattice. Am Mineral 35

Brigatti MF, Galan E, Theng BKG (2006) Structures and mineralogy of clay minerals. In: Bergaya F, Theng BKG, Lagal G (eds) Handbook of clay science. Elsevier Ltd

Bueno MJM, Gomez MJ, Herrera S, Hernando MD, Agüera A, Fernández-Alba AR (2012) Occurrence and persistence of organic emerging contaminants and priority pollutants in five sewage treatment plants of Spain: two years pilot survey monitoring. Environ Pollut 164:267–273. https://doi.org/10.1016/j.envpol.2012.01.038

Chang P-H, Li Z, Jiang W-T, Jean J-S (2009) Adsorption and intercalation of tetracycline by swelling clay minerals. Appl Clay Sci 46:27–36. https://doi.org/10.1016/j.clay.2009.07.002

Chang P-H, Li Z, Jean J-S, Jiang W-T, Wang C-J, Lin K-H (2012) Adsorption of tetracycline on 2:1 layered non-swelling clay mineral illite. Appl Clay Sci 67:158–163. https://doi.org/10.1016/j.clay.2011.11.004

Collins DR, Fitch AN, Catlow CRA (1992) Dehydration of vermiculites and montmorillonites: a time-resolved powder neutron diffraction study. J Mater Chem 2:865–873. https://doi.org/10.1039/JM9920200865

Daughton GC (2013) Pharmaceuticals in the environment: sources and their management. In: Petrovic M, Perez S, Barcelo D (eds) Analysis, removal, effects and risk of pharmaceuticals in the water cycle, 2nd edition, vol 62. Elsevier

de Jongh CM, Kooij PJ, de Voogt P, ter Laak TL (2012) Screening and human health risk assessment of pharmaceuticals and their transformation products in Dutch surface waters and drinking water. Sci Total Environ 427-428:70–77. https://doi.org/10.1016/j.scitotenv.2012.04.010

Dordio AV, Miranda S, Prates Ramalho JP, Carvalho AJP (2017) Mechanisms of removal of three widespread pharmaceuticals by

two clay materials. J Hazard Mater 323:575–583. https://doi.org/10.1016/j.jhazmat.2016.05.091

Eichhorn P (2013) General introduction on pharmaceuticals. In: Petrovic M, Perez S, Barcelo D (eds) Analysis, removal, effects and risk of pharmaceuticals in the water cycle, 2nd edition, vol 62. Elsevier

Fernandes C, Catrinescu C, Castilho P, Russo PA, Carrott MR, Breen C (2007) Catalytic conversion of limonene over acid activated Serra de Dentro (SD) bentonite. Appl Catal A Gen 318:108–120. https://doi.org/10.1016/j.apcata.2006.10.048

Ferrage E, Lanson B, Malikova N, Plançon A, Sakharov BA, Drits VA (2005) New insights on the distribution of interlayer water in bi-hydrated smectite from X-ray diffraction profile modeling of 00l reflections. Chem Mater 17:3499–3512. https://doi.org/10.1021/cm047995v

Ferrer I, Thurman EM (2013) Analysis of pharmaceuticals in drinking water, groundwater, surface water, and wastewater. In: Petrovic M, Perez S, Barcelo D (eds) Analysis, removal, effects and risk of pharmaceuticals in the water cycle, 2nd edition, vol 62. Elsevier

Földvári M (2011) Handbook of thermogravimetric system of minerals and its use in geological practice. Geological Institute of Hungary (=Magyar Állami Földtani Intézet)

Freundlich HMF (1906) Über die adsorption in läsungen. Z Phys Chem 57:385–470

Gupta VK, Ali I (2012) Environmental water: advances in treatment, remediation and recycling. Elsevier

Haul R (1982) S. J. Gregg, K. S. W. Sing: Adsorption, surface area and porosity. 2. Auflage, Academic Press, London 1982. 303 Seiten, Preis: $ 49.50. Ber Bunsenges Phys Chem 86:957–957. https://doi.org/10.1002/bbpc.19820861019

Ho YS (2004) Citation review of Lagergren kinetic rate equation on adsorption reactions. Scientometrics 59:171–177. https://doi.org/10.1023/B:SCIE.0000013305.99473.cf

Huo X, Wu L, Liao L, Xia Z, Wang L (2012) The effect of interlayer cations on the expansion of vermiculite. Powder Technol 224:241–246. https://doi.org/10.1016/j.powtec.2012.02.059

Jiang W-T, Chang P-H, Wang Y-S, Tsai Y, Jean J-S, Li Z, Krukowski K (2013) Removal of ciprofloxacin from water by birnessite. J Hazard Mater 250:362–369. https://doi.org/10.1016/j.jhazmat.2013.02.015

Jozefaciuk G, Muranyi A, Alekseeva T (2002) Effect of extreme acid and alkali treatment on soil variable charge. Geoderma 109:225–243. https://doi.org/10.1016/S0016-7061(02)00177-5

Kalinowski BE, Schweda P (2007) Rates and nonstoichiometry of vermiculite dissolution at 22°C. Geoderma 142:197–209. https://doi.org/10.1016/j.geoderma.2007.08.011

Kaviratna H, Pinnavaia TJ (1994) Acid hydrolysis of octahedral Mg^{2+} sites in 2:1 layered silicates: an assessment of edge attack and gallery access mechanisms. Clay Clay Miner 42:717–723

Kümmerer K (2008) Pharmaceuticals in the environment. Springer

Kunze GW (1965) Pretreatment for mineralogical analysis. In: Black CA (ed) Soil analysis. Part I. American Society of Agronomy, Wisconsin, pp 568–577

Kuzmanovic M, Banjac Z, Ginebreda A, Petrovic M, Barcelo D (2013) Prioritization: selection of environmentally occurring pharmaceuticals to be monitored. In: Petrovic M, Perez S, Barcelo D (eds) Analysis, removal, effects and risk of pharmaceuticals in the water cycle, 2nd edition, vol 62. Elsevier,

Lagergren S (1898) About theory of so-called adsorption of soluble substances. Kongl Vetenskaps Academiens Handlingar 24:1–39

Lajeunesse A, Smyth SA, Barclay K, Sauvé S, Gagnon C (2012) Distribution of antidepressant residues in wastewater and biosolids following different treatment processes by municipal wastewater treatment plants in Canada. Water Res 46:5600–5612. https://doi.org/10.1016/j.watres.2012.07.042

Lambropoulou D, Evgenidou E, Saliverou V, Kosma C, Konstantinou I (2017) Degradation of venlafaxine using TiO₂/UV process: kinetic studies, RSM optimization, identification of transformation products

and toxicity evaluation. J Hazard Mater 323:513–526. https://doi.org/10.1016/j.jhazmat.2016.04.074

Langmuir I (1918) The adsorption of gases on plane surfaces of glass, mica and platinum. J Am Chem Soc 40:1361–1403. https://doi.org/10.1021/ja02242a004

Li Z, Chang P-H, Jean J-S, Jiang W-T, Wang C-J (2010a) Interaction between tetracycline and smectite in aqueous solution. J Colloid Interface Sci 341:311–319. https://doi.org/10.1016/j.jcis.2009.09.054

Li Z, Schulz L, Ackley C, Fenske N (2010b) Adsorption of tetracycline on kaolinite with pH-dependent surface charges. J Colloid Interface Sci 351:254–260. https://doi.org/10.1016/j.jcis.2010.07.034

Li Z, Chang P-H, Jiang W-T, Jean J-S, Hong H, Liao L (2011) Removal of diphenhydramine from water by swelling clay minerals. J Colloid Interface Sci 360:227–232. https://doi.org/10.1016/j.jcis.2011.04.030

Li Z, Fitzgerald NM, Jiang W-T, Lv G (2016) Palygorskite for the uptake and removal of pharmaceuticals for wastewater treatment. Process Saf Environ Prot 101:80–87. https://doi.org/10.1016/j.psep.2015.09.008

Low MJD (1960) Kinetics of chemisorption of gases on solids. Chem Rev 60:267–312. https://doi.org/10.1021/cr60205a003

Marcos C, Argüelles A, Ruíz-Conde A, Sánchez-Soto PJ, Blanco JA (2003) Study of the dehydration process of vermiculites by applying a vacuum pressure: formation of interstratified phases. Mineral Mag 67:1253–1268. https://doi.org/10.1180/0026461036760163

Marcos C, Arango YC, Rodriguez I (2009) X-ray diffraction studies of the thermal behaviour of commercial vermiculites. Appl Clay Sci 42:368–378. https://doi.org/10.1016/j.clay.2008.03.004

Mareschal L, Ranger J, Turpault MP (2009) Stoichiometry of a dissolution reaction of a trioctahedral vermiculite at pH 2.7. Geochim Cosmochim Acta 73:307–319. https://doi.org/10.1016/j.gca.2008.09.036

Metcalfe CD, Chu S, Judt C, Li H, Oakes KD, Servos MR, Andrews DM (2010) Antidepressants and their metabolites in municipal wastewater, and downstream exposure in an urban watershed. Environ Toxicol Chem 29:79–89. https://doi.org/10.1002/etc.27

Papageorgiou M, Kosma C, Lambropoulou D (2016) Seasonal occurrence, removal, mass loading and environmental risk assessment of 55 pharmaceuticals and personal care products in a municipal wastewater treatment plant in Central Greece. Sci Total Environ 543:547–569. https://doi.org/10.1016/j.scitotenv.2015.11.047

Redlich O, Peterson DL (1959) A useful adsorption isotherm. J Phys Chem 63:1024–1024. https://doi.org/10.1021/j150576a611

Rivagli E, Pastorello A, Sturini M, Maraschi F, Speltini A, Zampori L, Setti M, Malavasi L, Profumo A (2014) Clay minerals for adsorption of veterinary FQs: behavior and modeling. J Environ Chem Eng 2:738–744. https://doi.org/10.1016/j.jece.2013.11.017

Ruiz-Conde A, Ruiz-Amil A, Perez-Rodriguez JL, Sanchez-Soto PJ (1996) Dehydration-rehydration in magnesium vermiculite: conversion from two-one and one-two water layer hydration states through the formation of interstratified phases. J Mater Chem 6:1557–1566. https://doi.org/10.1039/JM9960601557

Sakharov BA, Lindgreen H, Salyn AL, Drits VA (1999) Mixed-layer kaolinite-illite-vermiculite in North Sea shales. Clay Miner 34:333–334

Santos LH, Araujo AN, Fachini A, Pena A, Delerue-Matos C, Montenegro MC (2010) Ecotoxicological aspects related to the presence of pharmaceuticals in the aquatic environment. J Hazard Mater 175:45–95. https://doi.org/10.1016/j.jhazmat.2009.10.100

Schoonheydt RA, Johnston CT (2006) Surface and interface chemistry of clay minerals. In: Bergaya F, Theng BKG, Lagal G (eds) Handbook of clay science, vol 1. Elsevier

Schultz MM, Furlong ET (2008) Trace analysis of antidepressant pharmaceuticals and their select degradates in aquatic matrixes by LC/

ESI/MS/MS. Anal Chem 80:1756–1762. https://doi.org/10.1021/ac702154e

Sips R (1948) On the structure of a catalyst surface. J Chem Phys 16:490–495

Sposito G, Prost R (1982) Structure of water adsorbed on smectites. Chem Rev 82:553–573. https://doi.org/10.1021/cr00052a001

Stawiński W, Freitas O, Chmielarz L, Węgrzyn A, Komędera K, Błachowski A, Figueiredo S (2016) The influence of acid treatments over vermiculite based material as adsorbent for cationic textile dyestuffs. Chemosphere 153:115–129. https://doi.org/10.1016/j.chemosphere.2016.03.004

Stawiński W, Węgrzyn A, Dańko T, Freitas O, Figueiredo S, Chmielarz L (2017a) Acid-base treated vermiculite as high performance adsorbent: insights into the mechanism of cationic dyes adsorption, regeneration, recyclability and stability studies. Chemosphere 173:107–115. https://doi.org/10.1016/j.chemosphere.2017.01.039

Stawiński W, Węgrzyn A, Freitas O, Chmielarz L, Mordarski G, Figueiredo S (2017b) Simultaneous removal of dyes and metal cations using an acid, acid-base and base modified vermiculite as a sustainable and recyclable adsorbent. Sci Total Environ 576:398–408. https://doi.org/10.1016/j.scitotenv.2016.10.120

Stefanova RY (2001) Metal removal by thermally activated clay marl. Journal of environmental science and health Part A, Toxic/hazardous substances & environmental engineering 36:293–306

Styszko K, Nosek K, Motak M, Bester K (2015) Preliminary selection of clay minerals for the removal of pharmaceuticals, bisphenol A and triclosan in acidic and neutral aqueous solutions. C R Chim 18:1134–1142. https://doi.org/10.1016/j.crci.2015.05.015

Teng TT, Low LW (2012) Removal of dyes and pigments from industrial effluents. In: Sharma SK, Sanghi R (eds) Advances in water treatment and pollution prevention. Springer Netherlands

Thiebault T, Guégan R, Boussafir M (2015) Adsorption mechanisms of emerging micro-pollutants with a clay mineral: case of tramadol and doxepine pharmaceutical products. J Colloid Interface Sci 453:1–8. https://doi.org/10.1016/j.jcis.2015.04.029

Tóth J (1971) Acta Chimica Academiae Scientiarum Hungaricae 69

Tsai Y-L, Chang PH, Gao ZY, Xu XY, Chen YH, Wang ZH, Chen XY, Yang ZY, Wang TH, Jean JS, Li Z, Jiang WT (2016) Amitriptyline removal using palygorskite clay. Chemosphere 155:292–299. https://doi.org/10.1016/j.chemosphere.2016.04.062

Valcarcel Y, Gonzalez Alonso S, Rodriguez-Gil JL, Gil A, Catala M (2011) Detection of pharmaceutically active compounds in the rivers and tap water of the Madrid region (Spain) and potential ecotoxicological risk. Chemosphere 84:1336–1348. https://doi.org/10.1016/j.chemosphere.2011.05.014

Walker GF (1961) Vermiculite minerals. In: Brown G (ed) The X-ray identification and crystal structures of clay minerals. Mineral S Great Britain Monogr, Great Britain, pp 297–324

Wan M, Li Z, Hong H, Wu Q (2013) Enrofloxacin uptake and retention on different types of clays. J Asian Earth Sci 77:287–294. https://doi.org/10.1016/j.jseaes.2013.02.032

Wang C-J, Li Z, Jiang W-T (2011) Adsorption of ciprofloxacin on 2:1 dioctahedral clay minerals. Appl Clay Sci 53:723–728. https://doi.org/10.1016/j.clay.2011.06.014

Worch E (2012) Adsorption technology in water treatment: fundamentals, processes, and modeling. De Gruyter